On the orientation of molecular photofragments produced in highly excited rotational states

J. A. Beswick, M. GlassMaujean, and O. Roncero

Citation: J. Chem. Phys. **96**, 7514 (1992); doi: 10.1063/1.462403
View online: http://dx.doi.org/10.1063/1.462403
View Table of Contents: http://jcp.aip.org/resource/1/JCPSA6/v96/i10
Published by the American Institute of Physics.

On the orientation of molecular photofragments produced in highly excited rotational states

J. A. Beswick
LURE,[a] *Université de Paris Sud, 91405 Orsay, France*

M. Glass-Maujean
Laboratoire de Spectroscopie Hertzienne,[b] *Université Pierre et Marie Curie, 75252 Paris, France*

O. Roncero
Instituto de Fisica Fundamental, CSIC Serrano 123, 28006 Madrid, Spain

(Received 30 October 1991; accepted 17 January 1992)

The degree of orientation of highly excited rotational states of molecular fragments produced by photodissociation with circularly polarized light is studied quantum mechanically. It is shown that a significant orientation of the fragments' angular momentum **j** can be obtained when two or more dissociative continua correlated to the same final state of the products are excited simultaneously. In addition, the coherently excited continua should correspond to different helicity states, that is, to different projections of **j** on the reaction coordinate R (the vector joining the centers of mass of the fragments). The particular cases of an initial total angular momentum equal to zero as well as the axial recoil limit are discussed. The theory is applied to a simplified model of the photodissociation of ICN in the A continuum. The calculations have been performed by integration of the time independent quantum close-coupling equations for the coupling between the rotation of CN and the reaction coordinate R, using recently proposed potential energy surfaces and couplings. The results reproduce qualitatively the experimental results of Hasselbrink, Waldeck, and Zare [Chem. Phys. **126**, 191 (1988)], in particular, the change of sign and the large degree of orientation found for highly excited rotational states of the CN fragments.

I. INTRODUCTION

There has been growing interest in the last years on the study of vector properties such as the alignment and orientation of photofragment angular momenta in order to obtain the most detailed information on the dynamics of photodissociation.[1] Alignment and orientation of the fragment angular momentum **j** refer to a nonstatistical distribution of the population of the m_j sublevels associated to the projections of **j** on the space-fixed frame defined by the photon field. The degree of orientation is defined by the average value of m_j and hence it is zero when positive and negative m_j sublevels have equal populations. Because of symmetry, orientation of **j** can only be obtained by the use of circularly polarized light.

The first evidence for orientation of atomic fragments in the dissociation of diatomic molecules has been given by Vasyutinskii.[2] The oriented ground state cesium atoms produced in the photodissociation of CsI molecules by circularly polarized UV radiation were monitored by optical dichroism. More recently, oriented ground state Tl atoms were produced by dissociating TlBr and in this case it has been shown that nonadiabatic effects in the excited electronic states have a profound influence on the degree of orientation.[3]

Recently, the importance in this area of coherence effects due to simultaneous excitation of several continua has been demonstrated.[4–10] One particular striking example is the anomalous polarization of the $Ca^*(^1P)$ fluorescence observed in the photodissociation of Ca_2.[4,5] This effect is due to the interference between the emission from the coherently populated $\Lambda = \pm 1$ states in the dissociation through a Π electronic manifold. Consider a diatomic molecule AB excited by photon absorption to a dissociative $^1\Pi$ state leading to $A^*(^1P) + B(^1S)$ fragments. If the dissociation proceeds adiabatically, the excited $A^*(^1P)$ fragment will be populated exclusively in the magnetic sublevels $\Lambda = \pm 1$ and it is fully aligned in the molecular frame. Since the absorption probability has a $|\mathbf{d}\cdot\hat{\mathbf{e}}|^2$ dependence and **d** is strongly correlated to the internuclear axis **R** (for a diatomic molecule **d** is parallel to **R** for a $\Sigma \rightarrow \Sigma$ or $\Pi \rightarrow \Pi$ transition, and perpendicular to **R** for a $\Sigma \rightarrow \Pi$ transition), $A^*(^1P)$ is partially aligned in the space fixed frame even after averaging over all possible orientations of the internuclear axis. In addition, the fluorescence from the excited $A^*(^1P)$ fragment is dramatically affected by the interference between the emissions from the two coherently excited $\Lambda = \pm 1$ magnetic sublevels. In the case of Ca_2 for instance, the predicted degree of polarization is 0.78 (in good agreement with the experimental value) but it drops to a merely .14 if the interference terms are not taken into account.[4,5]

Other coherent excitation effects can also be of importance. Consider the case discussed above, namely, a mole-

[a] Laboratoire du CNRS, CEA et MEN.
[b] Laboratoire de l'ENS et de l'UPMC, associé au CNRS.

 0021-9606/92/107514-14$06.00

cule dissociating into $A^*(^1P) + B(^1S)$ fragments. Two molecular singlet states ($^1\Pi$ and $^1\Sigma$) are correlated to this limit. They can both be excited by optical absorption from a $^1\Sigma$ ground state and they will be coherently populated. Since the $^1\Pi$ state produces adiabatically $A^*(^1P,\Lambda = \pm 1)$ fragments while the $^1\Sigma$ state produces $A^*(^1P,\Lambda = 0)$ fragments, there will be an additional coherence between the $\Lambda = \pm 1,0$ sublevels. As opposed to the case discussed before, this coherence depends on the ratio of the photoabsorption amplitudes to the $^1\Sigma$ and $^1\Pi$ states as well as on the relative phase of their corresponding vibrational continuum wave functions. Recently, a quantum mechanical treatment of H_2 photodissociation in the region of the $C(^1\Pi)$, $B(^1\Sigma)$, and $B'(^1\Sigma)$ states has shown that these coherence effects can produce pronounced oscillations of the Ly_α fluorescence as a function of the excitation photon energy.[9]

All the examples discussed up to now concern diatomic molecules and therefore the alignment and orientation of the fragments' electronic angular momenta. Only very recently, rotational angular momentum orientation in a molecular photofragment has been observed.[11] By photolyzing ICN with circularly polarized light, Zare and co-workers have produced oriented CN fragments. It was found that the degree and sign of the orientation changes as a function of the rotational state N being considered. Low N states the orientation is positive, but for large N it becomes negative. It has been noted by Vigué *et al.*,[12] that the degree of orientation found in these experiments for large N correspond to an average value of $|\langle N_z\rangle| \simeq 7$ which is much larger than the unit angular momentum transferred to the molecule by the photon. An elegant model has been proposed by those authors to explain this unexpected result. The excited dissociative state (which corresponds to a Σ state in the collinear configuration) is assumed to acquire some mixed Π character due to the coupling with another state in the same energy region. The coupling is obviously zero at the collinear configuration but nonzero as the molecule bends. As a result of the mixing, it is possible to excite a coherent superposition of the $v = 0$ and $v = 1$ bending states which corresponds to a preferred sense of the rotation of CN within the ICN complex. This effect has been described as a vibronic angular momentum "amplification."[12]

Another mechanism for the production of a significant orientation of fragments in highly excited rotational states, has been considered by two of us.[10] It involves the coherent excitation of two dissociative states with different helicities (projection of $\mathbf{j}$ on the axis joining the centers of mass of the fragments), correlating to the same final state of the fragments. Very recently Yabushita and Morokuma[13] have performed *ab initio* calculations for the ICN molecule in the ground and in several excited electronic states. Based on these calculations they have proposed that two of their calculated excited electronic states (the $^3\Pi_0^+$ and the $^1\Pi_1$), both of them optically active from the ground state, should be directly involved in the dissociation of ICN in the A continuum. The two excited surfaces are bent and they undergo a conical intersection in the exit valley outside the Franck–Condon region. Since the two electronic states are coupled and have different symmetry, it is possible to excite two helicity states for each one of the final state of the fragments. Thus, according to our theory[10] the Yabushita and Morokuma potential scheme should also be able to explain the orientation of rotationally excited CN fragments found in the ICN experiment. It is the purpose of this paper to investigate numerically this question.

The organization of the paper is as follows. In Sec. II we present the standard quantum mechanical formulas for the orientation of photofragments[2,3,14–18] which apply to diatomics as well as to polyatomic molecules dissociating into two fragments, and we discuss the general conditions for obtaining oriented fragments in highly excited rotational states. In Secs. III and IV we study two simplifying limits, namely, the case where the initial state of the molecule corresponds to zero total angular momentum, and the axial recoil limit. In Sec. V we apply our general expressions to two different models for ICN and we compare with experiments. Finally, Sec. VI is devoted to the conclusions and, in particular, to the comparison between the different models presented in the literature as well as the possible ways in which they may be discriminated.

II. GENERAL THEORY

We shall consider a molecule dissociating into two fragments A and B and we shall denote by $\mathbf{R}$ the vector joining the two centers of mass. For simplicity, let us assume that only one fragment carries a nonzero angular momentum (electronic plus rotational), which we shall denote by $\mathbf{j}$. The general case of both fragments having nonzero angular momentum are presented in the Appendix. The general conclusions are not changed by this complication. The total angular momentum of the system is then given by

$$\mathbf{J} = \mathbf{j} + \mathbf{l}, \tag{1}$$

where $\mathbf{l} = (\hbar/i)\mathbf{R} \wedge \nabla_R$, is the orbital angular momentum associated to the relative motion of the fragments.

The degree of orientation $\mathcal{O}$ and alignment $\mathcal{A}$ (often also denoted by $A_0^{\{1\}}$ and $A_0^{\{2\}}$, respectively) are defined by[15]

$$\mathcal{O}^{(j)} \equiv \langle j_z/|\mathbf{j}|\rangle = \sum_{m_j} \frac{m_j}{\sqrt{j(j+1)}} \rho^{(j)}_{m_j,m_j}, \tag{2a}$$

$$\mathcal{A}^{(j)} \equiv \langle 3j_z^2/|\mathbf{j}|^2 - 1\rangle = \sum_{m_j} \left(\frac{3m_j^2}{j(j+1)} - 1\right)\rho^{(j)}_{m_j,m_j}, \tag{2b}$$

where m_j is the projection of $\mathbf{j}$ on the laboratory Z axis and $\rho^{(j)}_{m_j,m_j}$ is the final relative population of sublevel m_j with $\Sigma_{m_j}\rho^{(j)}_{m_j,m_j} = 1$. If we denote by $\sigma^{(j)}_{m_j}$ the partial photodissociation cross section for production of fragments in the particular level (j,m_j), we shall have

$$\rho^{(j)}_{m_j,m_j} = \sigma^{(j)}_{m_j} \Big/ \sum_{m_j} \sigma^{(j)}_{m_j}. \tag{3}$$

In the framework of the first-order perturbation theory for electric dipole transitions, the partial photodissociation cross section $\sigma^{(j)}_{m_j}$ is given by[16–18]

$$\sigma^{(j)}_{m_j} = \frac{4\pi^2\omega}{c} \sum_{l m_l} |\langle \Psi_{j m_j l m_l} | \mathbf{d}\cdot\hat{\mathbf{e}} | \Psi_i \rangle|^2, \tag{4}$$

where ω is the frequency of the incident light, $\hat{\mathbf{e}}$ its polariza-

tion vector, and $\mathbf{d}$ the electric dipole operator. In Eq. (4), Ψ_i is the initial molecular wave function, while $\Psi_{jm_j\ell m_\ell}$ is the final dissociative wave function, which as $R\to\infty$ behaves as

$$\Psi_{jm_j\ell m_\ell}(R\to\infty)\simeq\left(\frac{m}{2\pi k_j\hbar^2}\right)^{1/2}\left[\frac{e^{ik_jR}}{R}W^{\ell m_\ell}_{jm_j}(\mathbf{R},\{\mathbf{r}_{sf}\})+\sum_{j'm_{j'}}\sum_{\ell'm_{\ell'}}\left(\frac{k_j}{k_{j'}}\right)^{1/2}S^{*}_{jm_j\ell m_\ell,j'm_{j'}\ell'm_{\ell'}}\times\frac{e^{-ik_{j'}R}}{R}W^{\ell'm_{\ell'}}_{j'm_{j'}}(\mathbf{R},\{\mathbf{r}_{sf}\})\right],\quad(5)$$

where $\mathbf{S}$ is the scattering matrix, and

$$k_j=\sqrt{2m(E-E_j)}/\hbar\quad(6)$$

is the channel wave number, $m=m_Am_B/(m_A+m_B)$ is the reduced mass for the relative motion of the fragments, $E=E_i+\hbar\omega$ the total final energy, and E_j the asymptotic threshold energy. The channel basis set functions $W^{\ell m_\ell}_{jm_j}(\mathbf{R},\{\mathbf{r}_{sf}\})$ are defined as

$$W^{\ell m_\ell}_{jm_j}\mathbf{R},\{\mathbf{r}_{sf}\})=Y_{\ell m_\ell}(\theta_{\mathbf{R}},\phi_{\mathbf{R}})\phi_{jm_j}(\{\mathbf{r}_{sf}\};R),\quad(7)$$

where the $Y_{\ell m_\ell}(\theta_{\mathbf{R}},\phi_{\mathbf{R}})$ are spherical harmonic functions depending on the polar angles of $\mathbf{R}$, and the $\phi_{jm_j}(\{\mathbf{r}_{sf}\};R)$ are adiabatic basis functions which asymptotically (i.e., for $R\to\infty$) become eigenfunctions of the fragments. We have denoted by $\{\mathbf{r}_{sf}\}$ the collection of all space-fixed (sf) coordinates (electronic, vibrational, and rotational) of the fragments.

In molecular photofragmentation problems it is usually more convenient to calculate the matrix elements of the dipole operator $\mathbf{d}$ in a body-fixed (bf) frame with the z axis pointing in the direction of $\mathbf{R}$. As $R\to\infty$, the projection of $\mathbf{J}$ on this axis (the helicity quantum number Ω) becomes well defined and the continuum wave functions behave as

$$\Psi_{j\Omega JM}(R\to\infty)\simeq\left(\frac{m}{2\pi k_j\hbar^2}\right)^{1/2}\left[\frac{e^{ik_jR}}{R}W^{JM}_{j\Omega}(\mathbf{R},\{\mathbf{r}_{bf}\})+\sum_{j'\Omega'}\left(\frac{k_j}{k_{j'}}\right)^{1/2}S^{(J)*}_{j\Omega,j'\Omega'}\frac{e^{-ik_{j'}R}}{R}\times W^{JM}_{j'\Omega'}(\mathbf{R},\{\mathbf{r}_{bf}\})\right],\quad(8)$$

with

$$W^{JM}_{j\Omega}(\mathbf{R},\{\mathbf{r}_{bf}\})=\sqrt{\frac{2J+1}{4\pi}}\,D^{J*}_{M\Omega}(\phi_R,\theta_R,0)\phi_{j\Omega}(\{\mathbf{r}_{bf}\};R),\quad(9)$$

where the $D^{J*}_{M\Omega}(\phi_R,\theta_R,0)$ are Wigner rotational functions and M is the projection of $\mathbf{J}$ on the space-fixed Z axis. Notice that $\phi_{j\Omega}(\{\mathbf{r}_{bf}\};R)$ refer now to the body-fixed frame. Since between the space-fixed and the body-fixed basis set there is the relationship[16]

$$Y_{\ell m_\ell}(\theta_R,\phi_R)\phi_{jm_j}(\{\mathbf{r}_{sf}\};R)=\sum_{\Omega JM}(-)^{M-\Omega}(2\ell+1)^{1/2}\frac{(2J+1)}{\sqrt{4\pi}}\times\begin{pmatrix}j&\ell&J\\\Omega&0&-\Omega\end{pmatrix}\begin{pmatrix}j&\ell&J\\m_j&m_\ell&-M\end{pmatrix}\times D^{J*}_{M\Omega}(\phi_R,\theta_R,0)\phi_{j\Omega}(\{\mathbf{r}_{bf}\};R),\quad(10)$$

we can write

$$\Psi_{jm_j\ell m_\ell}=\sum_{\Omega JM}\mathcal{T}^{jm_j\ell m_\ell}_{\Omega JM}\Psi_{j\Omega JM},\quad(11)$$

with

$$\mathcal{T}^{jm_j\ell m_\ell}_{\Omega JM}=(-)^{M-\Omega}(2\ell+1)^{1/2}(2J+1)^{1/2}\times\begin{pmatrix}j&\ell&J\\\Omega&0&-\Omega\end{pmatrix}\begin{pmatrix}j&\ell&J\\m_j&m_\ell&-M\end{pmatrix}.\quad(12)$$

Introduction of Eq. (11) into Eq. (4) produces

$$\sigma^{(j)}_{m_j}=\frac{4\pi^2\omega}{c}\sum_{\ell m_\ell}\sum_{\Omega JM}\sum_{\Omega'J'M'}\mathcal{T}^{jm_j\ell m_\ell}_{\Omega JM}\mathcal{T}^{jm_j\ell m_\ell}_{\Omega'J'M'}\times\langle\Psi_i|\mathbf{d}\cdot\hat{\mathbf{e}}|\Psi_{j\Omega JM}\rangle^{*}\langle\Psi_i|\mathbf{d}\cdot\hat{\mathbf{e}}|\Psi_{j\Omega'J'M'}\rangle,\quad(13)$$

which using Eq. (12) can be recast in the form (see Appendix A)

$$\sigma^{(j)}_{m_j}=\frac{4\pi^2\omega}{c}\sum_K(-)^{j-m_j}\frac{(2K+1)}{\sqrt{2j+1}}\begin{pmatrix}j&j&K\\m_j&-m_j&0\end{pmatrix}T^{(j)}_K,\quad(14)$$

with

$$T^{(j)}_K=\sum_{\Omega J}\sum_{\Omega'J'}\sum_M(-)^{j+M+K}(2j+1)^{1/2}\times\begin{pmatrix}j&j&K\\-\Omega'&\Omega&\Omega'-\Omega\end{pmatrix}(2J+1)^{1/2}(2J'+1)^{1/2}\times\begin{pmatrix}J&J'&K\\-\Omega&\Omega'&\Omega-\Omega'\end{pmatrix}\begin{pmatrix}J'&J&K\\-M&M&0\end{pmatrix}\times\langle\Psi_i|\mathbf{d}\cdot\hat{\mathbf{e}}|\Psi_{j\Omega JM}\rangle^{*}\langle\Psi_i|\mathbf{d}\cdot\hat{\mathbf{e}}|\Psi_{j\Omega'J'M'}\rangle\quad(15)$$

being the so-called state multipoles.[14,15,19]

Several comments concerning Eqs. (14) and (15) are now in order. From the form given to $\sigma^{(j)}_{m_j}$ in Eq. (14), it is easy to show that

$$\sigma^{(j)}\equiv\sum_{m_j}\sigma^{(j)}_{m_j}=\frac{4\pi^2\omega}{c}T^{(j)}_0,\quad(16a)$$

$$\mathcal{O}^{(j)}=\frac{T^{(j)}_1}{T^{(j)}_0},\quad(16b)$$

$$\mathcal{A}^{(j)}=\sqrt{\frac{(2j+3)(2j-1)}{j(j+1)}}\,\frac{T^{(j)}_2}{T^{(j)}_0},\quad(16c)$$

and therefore the state multipoles $T^{(j)}_K$ are directly related to the partial cross section ($K=0$), the degree of orientation ($K=1$), and the degree of alignment ($K=2$) of the rotational state j. For instance, using Eq. (15) with $K=0$ into Eq. (16a) it is obtained

$$\sigma^{(j)} = \frac{4\pi^2\omega}{c} \sum_{\Omega J M} |\langle \Psi_i | \mathbf{d}\cdot\hat{\mathbf{e}} | \Psi_{j\Omega JM} \rangle|^2, \tag{17}$$

which indeed is the partial photodissociation cross section for production of fragments with angular momentum equal to j, expressed in terms of spherical waves in the body-fixed frame.[16]

Similarly, using Eq. (15) with $K = 1$ into Eq. (16b) one gets

$$\mathcal{O}^{(j)} = -\sum_{\Omega J} \sum_{\Omega' J'} (-)^j (2j+1)^{1/2} \begin{pmatrix} j & j & 1 \\ -\Omega' & \Omega & \Omega' - \Omega \end{pmatrix} (2J+1)^{1/2} (2J'+1)^{1/2} \begin{pmatrix} J & J' & 1 \\ -\Omega & \Omega' & \Omega - \Omega' \end{pmatrix} \times \left[\frac{\Sigma_M (-1)^M \begin{pmatrix} J' & J & 1 \\ -M & M & 0 \end{pmatrix} \langle \Psi_i | \mathbf{d}\cdot\hat{\mathbf{e}} | \Psi_{j\Omega JM} \rangle^* \langle \Psi_i | \mathbf{d}\cdot\hat{\mathbf{e}} | \Psi_{j\Omega' J' M'} \rangle}{\Sigma_{\Omega JM} |\langle \Psi_i | \mathbf{d}\cdot\hat{\mathbf{e}} | \Psi_{j\Omega JM} \rangle|^2} \right], \tag{18}$$

which vanishes if only one state with $\Omega = 0$ is excited.[2,3] For a diatomic molecule this would correspond to a Σ dissociative state. In this work we are interested in the limit of large j. If only one excited state with $\Omega \neq 0$ is populated, then from

$$(2j+1)^{1/2} \begin{pmatrix} j & j & 1 \\ -\Omega & \Omega & 0 \end{pmatrix} = -(-)^{j+\Omega} \frac{\Omega}{\sqrt{j(j+1)}} \tag{19}$$

we conclude that the degree of orientation should vanish roughly as $1/j$. We thus expect very little orientation for large j when only one helicity manifold is excited. On the contrary, if two (or more) helicities with $\Delta\Omega = \pm 1$ are excited simultaneously from the same initial state (coherent excitation), we shall have terms in Eq. (18) involving coefficients of the form

$$(2j+1)^{1/2} \begin{pmatrix} j & j & 1 \\ -\Omega - 1 & \Omega & 1 \end{pmatrix} = -(-)^{j+\Omega} \sqrt{\frac{(j-\Omega)(j+\Omega+1)}{2j(j+1)}}, \tag{20}$$

which for j much larger than Ω approaches a constant value $1/\sqrt{2}$. We conclude that highly oriented molecular fragments such as those observed by Hasselbrink, Waldeck, and Zare in the photodissociation of ICN,[11] can be produced only if two or more helicity states are excited simultaneously. It is interesting to note that this result is not restricted to electric dipole transitions. Equations (14) and (15) are still valid if the electric dipole interaction term $\mathbf{d}\cdot\hat{\mathbf{e}}$ is replaced by another transition operator.

We now go back to Eq. (15) and specify further the wave functions needed to calculate the matrix elements of the transition dipole operator. We expand the final dissociative wave functions $\Psi_{j\Omega JM}$ in terms of the basis set given in Eq. (9),

$$\Psi_{j\Omega JM} = \frac{1}{R} \sum_{j'\Omega'} \varphi^{(J)}_{j\Omega, j'\Omega'}(R) W^{JM}_{j\Omega}(\mathbf{R}, \{\mathbf{r}_{\rm bf}\}). \tag{21}$$

Introducing this expansion into the Schrödinger equation it is found that the $\varphi^{(J)}_{j\Omega, j'\Omega'}$ functions are the solutions of the system of coupled equations,

$$\left[-\frac{\hbar^2}{2m} \frac{\partial^2}{\partial R^2} - \frac{\hbar^2 [J(J+1) + j(j+1) - 2\Omega^2]}{2mR^2} + V^{(J)}_{j\Omega, j\Omega}(R) - E_j - E \right] \varphi^{(J)}_{j\Omega, j\Omega}(R) = -\sum_{j'} V^{(J)}_{j\Omega, j'\Omega}(R) \varphi^{(J)}_{j\Omega, j'\Omega}(R) - \sum_{\Omega' = \Omega \pm 1} \left(\frac{\hbar^2}{2mR^2} \right) \sqrt{J(J+1) - \Omega\Omega'} \sqrt{j(j+1) - \Omega\Omega'} \varphi^{(J)}_{j\Omega, j\Omega'}(R), \tag{22}$$

with the asymptotic boundary condition [see Eq. (8)]

$$\varphi^{(J)}_{j\Omega, j'\Omega'}(R \to \infty) \simeq \left(\frac{m}{2\pi k_j \hbar^2} \right)^{1/2} \times \left[e^{ik_j R} \delta_{\Omega\Omega'} \delta_{jj'} + \left(\frac{k_j}{k_{j'}} \right)^{1/2} S^{(J)*}_{j\Omega, j'\Omega'} e^{-ik_{j'} R} \right]. \tag{23}$$

It should be noted that in Eqs. (22) the V terms include both potential and nonadiabatic interactions.

Similarly, it is convenient to expand the initial eigenstate Ψ_i in terms of the same molecule-fixed rotational basis set,

$$\Psi_{J_i M_i} = \frac{1}{R} \sum_{j_i \Omega_i} \varphi^{(J_i)}_{j_i \Omega_i}(R) W^{j_i M_i}_{j_i \Omega_i}(\mathbf{R}, \{\mathbf{r}_{\rm bf}\}), \tag{24}$$

with the $\varphi^{(J_i)}_{j_i \Omega_i}$ being determined by a system of coupled equations similar to Eqs. (22).

Using Eqs. (21) and (24), the matrix elements of the electric dipole operator will be given by

$$\langle \Psi_{J_i M_i} | \mathbf{d}\cdot\hat{\mathbf{e}} | \Psi_{j\Omega JM} \rangle = \sum_{p=0,\pm 1} (-)^{J_i - M_i - p} \times (2J_i + 1)^{1/2} (\hat{\mathbf{e}})_p \times \begin{pmatrix} J & 1 & J_i \\ M & -p & -M_i \end{pmatrix} \langle J_i \| \mathbf{d} \| j\Omega J \rangle, \tag{25}$$

where we have defined the reduced matrix elements

$$\langle J_i \| \mathbf{d} \| j\Omega J \rangle = \sum_{j_i\Omega_i} \sum_{j'\Omega'} (-)^{J_i - \Omega_i} (2J+1)^{1/2} \times \begin{pmatrix} J & 1 & J_i \\ \Omega' & \Omega_i - \Omega' & -\Omega_i \end{pmatrix} \int dR\, \varphi_{j_i\Omega_i}^{(J_i)*}(R) \times \langle \phi_{j_i\Omega_i} | (\mathbf{d})_{\Omega_i - \Omega'} | \phi_{j'\Omega'} \rangle \varphi_{j\Omega, j'\Omega'}^{(J)}(R). \quad (26)$$

In Eq. (25),

$$(\hat{\mathbf{e}})_0 = (\hat{\mathbf{e}})_Z, \quad (\hat{\mathbf{e}})_{\pm 1} = \mp \frac{1}{\sqrt{2}} [(\hat{\mathbf{e}})_X \pm i(\hat{\mathbf{e}})_Y] \quad (27)$$

are the tensorial components of the polarization vector in the space-fixed frame. In Eq. (26) on the other hand,

$$(\mathbf{d})_0 = (\mathbf{d})_z, \quad (\mathbf{d})_{\pm 1} = \mp \frac{1}{\sqrt{2}} [(\mathbf{d})_x \pm i(\mathbf{d})_y] \quad (28)$$

are the components of the electric dipole operator in the molecule-fixed frame.

Introducing Eq. (28) into Eq. (15) and averaging over M_i assuming the molecule is initially randomly oriented, one obtains (see Appendix)

$$T_K^{(j)} = -\left[\sum_p (-)^{1-p} |\hat{\mathbf{e}}_p|^2 \begin{pmatrix} 1 & 1 & K \\ p & -p & 0 \end{pmatrix}\right] \sum_{\Omega J} \sum_{\Omega' J'} (-)^{j - J_i} (2j+1)^{1/2} \begin{pmatrix} j & j & K \\ -\Omega' & \Omega & \Omega' - \Omega \end{pmatrix} (2J+1)^{1/2} \times (2J'+1)^{1/2} \begin{pmatrix} J & J' & K \\ \Omega & -\Omega' & \Omega' - \Omega \end{pmatrix} \begin{Bmatrix} 1 & 1 & K \\ J & J' & J_i \end{Bmatrix} \langle J_i \| \mathbf{d} \| j\Omega J \rangle^* \langle J_i \| \mathbf{d} \| j\Omega' J' \rangle, \quad (29)$$

which is the standard expression for the state multipoles in the case of electric dipole transitions.[2,3,6,7,14,15] Let us denote by

$$F_K(\hat{\mathbf{e}}) = \sum_p (-)^{1-p} |\hat{\mathbf{e}}_p|^2 \begin{pmatrix} 1 & 1 & K \\ p & -p & 0 \end{pmatrix} \quad (30)$$

the term within brackets in Eq. (29) which depends only on the polarization of the incident light. From the Wigner coefficient it is clear that K can only take the values 0, 1, and 2 which is the expected result in the case of electric dipole transitions in randomly oriented molecules. The actual values of F_K are

$$F_0(\hat{\mathbf{e}}) = \frac{1}{\sqrt{3}}, \quad (31a)$$

$$F_1(\hat{\mathbf{e}}) = \sum_p \frac{p}{\sqrt{6}} |\hat{\mathbf{e}}_p|^2, \quad (31b)$$

$$F_2(\hat{\mathbf{e}}) = \sum_p \frac{3p^2 - 2}{\sqrt{30}} |\hat{\mathbf{e}}_p|^2. \quad (31c)$$

For linear incident polarized light one can choose the laboratory Z axis in the direction of $\hat{\mathbf{e}}$ and we get

$$F_1(\hat{\mathbf{e}}) = 0, \quad (32a)$$

$$F_2(\hat{\mathbf{e}}) = -2/\sqrt{30}. \quad (32b)$$

For circular polarization on the other hand, it is convenient to choose the laboratory Z axis along the direction of propagation of the light. One then has $\hat{\mathbf{e}} = \mp (1/\sqrt{2})(\hat{\mathbf{e}}_X \mp i\hat{\mathbf{e}}_Y$ and

$$F_1(\hat{\mathbf{e}}) = \pm 1/\sqrt{6}, \quad (33a)$$

$$F_2(\hat{\mathbf{e}}) = 1/\sqrt{30}. \quad (33b)$$

It is then clear from Eqs. (32) and (33) that orientation ($K = 1$) can be produced only by the use of circularly (or elliptically) polarized light.[19] This is a well-known fact also in the case of photoionization where circularly polarized light is used to produce polarized (spin oriented) electrons.[20,21]

III. ZERO INITIAL TOTAL ANGULAR MOMENTUM

Let us consider the particular case $J_i = 0$. Only final states with $J = 1, \Omega = 0, \pm 1$ will be excited in that case. From Eq. (26) we have

$$\langle J_i = 0 \| \mathbf{d} \| j\Omega J = 1 \rangle = (-)^{1-\Omega} M_\Omega^{(j)}, \quad (34)$$

where

$$M_\Omega^{(j)} = \sum_{j'\Omega'} \sum_{j_i} (-)^{\Omega - \Omega'} \int dR\, \varphi_{j_i\Omega_i = 0}^{(J_i = 0)*}(R) \times \langle \phi_{j_i\Omega_i = 0} | (\mathbf{d})_{-\Omega'} | \phi_{j'\Omega'} \rangle \varphi_{j\Omega, j'\Omega'}^{(J=1)}(R). \quad (35)$$

Using Eq. (34) into (29), we obtain

$$T_K^{(j)} = -F_K(\hat{\mathbf{e}}) \sum_{\Omega\Omega'} (-)^{j+K-\Omega-\Omega'} (2j+1)^{1/2} \times \begin{pmatrix} j & j & K \\ -\Omega' & \Omega & \Omega' - \Omega \end{pmatrix} \times \begin{pmatrix} 1 & 1 & K \\ \Omega & -\Omega' & \Omega' - \Omega \end{pmatrix} M_\Omega^{(j)*} M_{\Omega'}^{(j)}, \quad (36)$$

where the F_K functions are defined in Eqs. (30) and (31). Using Eq. (36) into Eqs. (16), we finally get

$$\sigma^{(j)} = \frac{4\pi^2\omega}{3c} \{|M_0^{(j)}|^2 + |M_{1^{(+)}}^{(j)}|^2 + |M_{1^{(-)}}^{(j)}|^2\}, \quad (37a)$$

$$\mathscr{O}^{(j)} = \frac{1}{2} \left(\sum_p p|\hat{\mathbf{e}}|^2\right) \left\{ \frac{|M_{1^{(+)}}^{(j)}|^2 + |M_{1^{(-)}}^{(j)}|^2}{\sqrt{j(j+1)}} - (M_0^{(j)*} M_{1^{(+)}}^{(j)} + \text{c.c.}) \right\} \Big/ \{|M_0^{(j)}|^2 + |M_{1^{(+)}}^{(j)}|^2 + |M_{1^{(-)}}^{(j)}|^2\}, \quad (37b)$$

$$\mathscr{A}^{(j)} = \frac{1}{10}\left(\sum_p (3p^2-2)|\hat{\mathbf{e}}|^2\right)\left\{2|M_0^{(j)}|^2 + \left(\frac{3}{j(j+1)} + 2\right)|M_{1(+)}^{(j)}|^2 + \left(\frac{3}{j(j+1)} - 4\right)|M_{1(-)}^{(j)}|^2 - \frac{3}{\sqrt{j(j+1)}}(M_0^{(j)*}M_{1(+)}^{(j)} + \text{c.c.})\right\} \times\{|M_0^{(j)}|^2 + |M_{1(+)}^{(j)}|^2 + |M_{1(-)}^{(j)}|^2\}, \quad (37c)$$

where we have defined the parity adapted matrix elements for a $J_i = 0 \to J = 1$ transition,

$$M_{1(\pm)}^{(j)} = \frac{1}{\sqrt{2}}(M_{-1}^{(j)} \pm M_1^{(j)}). \quad (38)$$

We now turn to the study of orientation in the high j limit. From Eq. (37b) we obtain for circularly polarized light

$$\mathscr{O}^{(j)} = \mp\frac{1}{2}\left\{\frac{M_0^{(j)*}M_{1(+)}^{(j)} + \text{c.c.}}{|M_0^{(j)}|^2 + |M_{1(+)}^{(j)}|^2 + |M_{1(-)}^{(j)}|^2}\right\}, \quad (39)$$

where the two signs refer to right and left polarization, respectively. As discussed above in relation to Eq. (18) we note that for large j, orientation can be obtained only if two helicity states are excited simultaneously. In the case studied here we see that $M_0^{(j)}$ and $M_{1(+)}^{(j)}$ have to be coherently excited in order to obtain a nonvanishing orientation. This corresponds to the excitation of the two transition dipole moments perpendicular to j (in the case of a triatomic, this would correspond to the excitation of two transitions in the plane of the molecule, i.e., two parallel transitions). We note from Eq. (39) that the orientation can be as large as $\frac{1}{2}$ for $M_0^{(j)} = M_{1(+)}^{(j)}$ and $M_{1(-)}^{(j)} = 0$. Since $\langle j_Z\rangle = j\mathscr{O}^{(j)}$ and $j \gg 1$, we can then obtain $|\langle j_Z\rangle| \gg 1$.

It is also interesting to analyze the alignment in the limit $j \gg 1$. For linear incident polarization, we get from Eq. (37c)

$$\mathscr{A}^{(j)} = -\frac{2}{5}\left\{\frac{|M_0^{(j)}|^2 + |M_{1(+)}^{(j)}|^2 - 2|M_{1(-)}^{(j)}|^2}{|M_0^{(j)}|^2 + |M_{1(+)}^{(j)}|^2 + |M_{1(-)}^{(j)}|^2}\right\} \quad (40)$$

and we find that $\mathscr{A}^{(j)} = -\frac{2}{5}$ if $M_{1(-)}^{(j)} = 0$, while $\mathscr{A}^{(j)} = \frac{4}{5}$ if $M_0^{(j)} = M_{1(+)}^{(j)} = 0$, which are the limiting values of the alignment.[14,15] This result is also expected in the framework of the classical model. Since $j \gg 1$, and $J \ll j$, we shall have $\mathbf{l} \simeq -\mathbf{j}$ and therefore $\mathbf{j}$ is perpendicular to $\mathbf{R}$. Now for large j, $M_0^{(j)}$ and $M_{1(+)}^{(j)}$ correspond to a parallel transition, i.e., to a transition dipole moment in the plane perpendicular to $\mathbf{j}$ and containing $\mathbf{R}$ (the plane of the molecule for a triatomic), while $M_{1(-)}^{(j)}$ correspond to a transition dipole moment along $\mathbf{j}$ (i.e., perpendicular to the plane of the molecule in the triatomic case). We shall then have for linear polarization along the laboratory Z axis (see Fig. 1)

$$\mathbf{M}\cdot\hat{\mathbf{e}} = M_0^{(j)}\cos\Theta + M_{1(+)}^{(j)}\sin\Theta\cos\Phi + M_{1(-)}^{(j)}\sin\Theta\sin\Phi \quad (41)$$

and the absorption probability will be

$$dW_{\text{abs}} = \frac{3}{4\pi}\frac{|M_0^{(j)}\cos\Theta + M_{1(+)}^{(j)}\sin\Theta\cos\Phi + M_{1(-)}^{(j)}\sin\Theta\sin\Phi|^2}{|M_0^{(j)}|^2 + |M_{1(+)}^{(j)}|^2 + |M_{1(-)}^{(j)}|^2}\, d(\cos\Theta)d\Phi. \quad (42)$$

Since $\mathscr{A}^{(j)} = \langle 3j_Z^2/j^2 - 1\rangle$ and in the classical limit $j_Z = j\sin\Theta\sin\Phi$, we obtain

$$\mathscr{A}^{(j)} = 3\int dW_{\text{abs}}\sin\Theta^2\sin\Phi^2 - 1 = -\frac{2}{5}\left\{\frac{|M_0^{(j)}|^2 + |M_{1(+)}^{(j)}|^2 - 2|M_{1(-)}^{(j)}|^2}{|M_0^{(j)}|^2 + |M_{1(+)}^{(j)}|^2 + |M_{1(-)}^{(j)}|^2}\right\}, \quad (43)$$

which is exactly the result obtained in Eq. (40) using the quantum formalism.

IV. AXIAL RECOIL LIMIT

When J_i is different from zero, the general form Eq. (29) together with Eq. (26) should be used to calculate the multipoles $T_K^{(j)}$ from which the orientation and alignment can be obtained by the use of Eq. (16). Equation (29) can be simplified, however, for direct dissociation with large kinetic energies. In this limit (called axial recoil) the molecule dissociates much faster than the time for an overall rotation. This amounts to consider that the dissociation matrix elements Eq. (26) are slowly varying functions of the total angular momentum J and that Ω is a good quantum number. Therefore we shall write

$$\langle J_i\|\mathbf{d}\|j\Omega J\rangle = \sum_{\Omega_i}(-)^{J_i-\Omega_i}(2J+1)^{1/2}\begin{pmatrix} J & 1 & J_i \\ \Omega & (\Omega_i-\Omega) & -\Omega_i\end{pmatrix}\mathscr{M}_\Omega^{(j)}(J_i,\Omega_i), \quad (44)$$

where

$$\mathscr{M}_\Omega^{(j)}(J_i,\Omega_i) = \sum_{j_i}\sum_{j'}\int dR\,\varphi_{j\Omega_i}^{(J_i)*}(R) \times\langle\phi_{j_i\Omega_i}|(\mathbf{d})_{\Omega_i-\Omega}|\phi_{j'\Omega}\rangle\varphi_{j\Omega,j'\Omega}^{(J)}(R), \quad (45)$$

where J can be replaced by any of the three values $J = J_i$, $J_i \pm 1$. Introducing Eq. (44) into Eq. (29) one obtains (see Appendix)

$$T_K^{(j)} = -F_K(\hat{\mathbf{e}})\sum_{\Omega\Omega'}\sum_{\Omega_i}(-)^{j+\Omega+\Omega'-\Omega_i}(2j+1)^{1/2} \times\begin{pmatrix} j & j & K \\ -\Omega & \Omega' & (\Omega-\Omega')\end{pmatrix} \times\begin{pmatrix} 1 & 1 & K \\ (\Omega_i-\Omega') & (\Omega-\Omega_i) & (\Omega'-\Omega)\end{pmatrix} \times\mathscr{M}_\Omega^{(j)*}(\Omega_i,J_i)\mathscr{M}_{\Omega'}^{(j)}(\Omega_i,J_i), \quad (46)$$

where $F_K(\hat{\mathbf{e}})$ has been defined in Eqs. (30) and (31).

Using now Eq. (46) into Eqs. (16a) we obtain

$$\sigma^{(j)} = \frac{4\pi^2\omega}{3c} \sum_{\Omega_i} \{|\mathcal{M}^{(j)}_{\Omega_i}|^2 + |\mathcal{M}^{(j)}_{\Omega_i+1}|^2 + |\mathcal{M}^{(j)}_{\Omega_i-1}|^2\}, \tag{47a}$$

$$\mathcal{O}^{(j)} = \frac{1}{2}\left(\sum_p p|\hat{\mathbf{e}}|^2\right) \sum_{\Omega_i} \left\{ \frac{(1+\Omega_i)|\mathcal{M}^{(j)}_{\Omega_i+1}|^2 + (1-\Omega_i)|\mathcal{M}^{(j)}_{\Omega_i-1}|^2}{\sqrt{j(j+1)}} - \sqrt{\frac{(j-\Omega_i)(j+\Omega_i+1)}{2j(j+1)}} (\mathcal{M}^{(j)*}_{\Omega_i}\mathcal{M}^{(j)}_{\Omega_i+1} + \text{c.c.}) - \sqrt{\frac{(j+\Omega_i)(j-\Omega_i+1)}{2j(j+1)}} (\mathcal{M}^{(j)*}_{\Omega_i}\mathcal{M}^{(j)}_{\Omega_i-1} + \text{c.c.}) \right\} \Bigg/ \sum_{\Omega_i} \{|\mathcal{M}^{(j)}_{\Omega_i}|^2 + |\mathcal{M}^{(j)}_{\Omega_i+1}|^2 + |\mathcal{M}^{(j)}_{\Omega_i-1}|^2\}, \tag{47b}$$

$$\mathcal{A}^{(j)} = \frac{1}{10}\left(\sum_p (3p^2-2)|\hat{\mathbf{e}}|^2\right) \sum_{\Omega_i} \left\{ -2\left(\frac{3\Omega_i^2}{j(j+1)} - 1\right)|\mathcal{M}^{(j)}_{\Omega_i}|^2 + \left(\frac{3(\Omega_i+1)^2}{j(j+1)} - 1\right)|\mathcal{M}^{(j)}_{\Omega_i+1}|^2 + \left(\frac{3(\Omega_i-1)^2}{j(j+1)} - 1\right)|\mathcal{M}^{(j)}_{\Omega_i-1}|^2 - \frac{3(2\Omega_i+1)}{j(j+1)}\sqrt{(j-\Omega_i)(j+\Omega_i+1)} \times \left[\frac{\mathcal{M}^{(j)*}_{\Omega_i}\mathcal{M}^{(j)}_{\Omega_i+1} + \text{c.c.}}{\sqrt{2}}\right] + \frac{3(2\Omega_i-1)}{j(j+1)}\sqrt{(j-\Omega_i+1)(j+\Omega_i)} \times \left[\frac{\mathcal{M}^{(j)*}_{\Omega_i}\mathcal{M}^{(j)}_{\Omega_i-1} + \text{c.c.}}{\sqrt{2}}\right] + \frac{3}{j(j+1)} \times \sqrt{(j+\Omega_i+1)(j+\Omega_i)(j-\Omega_i+1)(j-\Omega_i)}\,[\mathcal{M}^{(j)*}_{\Omega_i+1}\mathcal{M}^{(j)}_{\Omega_i-1} + \text{c.c.}] \right\} \Bigg/ \sum_{\Omega_i} \{|\mathcal{M}^{(j)}_{\Omega_i}|^2 + |\mathcal{M}^{(j)}_{\Omega_i+1}|^2 + |\mathcal{M}^{(j)}_{\Omega_i-1}|^2\}, \tag{47c}$$

which reduce to Eqs. (37) for the particular case $J_i = 0$ if only one term $\Omega_i = 0$ is considered (notice, however, that the M and $\mathcal{M}$ matrix elements have slightly different definitions and they become identical for $J_i = 0$ only if the Coriolis coupling between different Ω states are neglected). Another consequence of the axial recoil approximation is that the degree of orientation given in Eq. (47b) vanishes if $\mathcal{M}_{\Omega_i \pm 1} = 0$ even for $\mathcal{M}_{\Omega_i} \neq 0$ (parallel transition). Thus in the axial recoil limit, orientation of j can only be obtained if some perpendicular transition dipole moment is different from zero. Moreover, for $j \gg 1$ and circularly polarized incident light we obtain from Eq. (47b)

$$\mathcal{O}^{(j)} = \mp\frac{1}{2}\left\{\frac{\Sigma_{\Omega_i}\left[\mathcal{M}^{(j)*}_{\Omega_i}\mathcal{M}^{(j)}_{\Omega_i+1} + \mathcal{M}^{(j)*}_{\Omega_i}\mathcal{M}^{(j)}_{\Omega_i-1} + \text{c.c.}\right]}{\sqrt{2}\Sigma_{\Omega_i}\left[|\mathcal{M}^{(j)}_{\Omega_i}|^2 + |\mathcal{M}^{(j)}_{\Omega_i+1}|^2 + |\mathcal{M}^{(j)}_{\Omega_i-1}|^2\right]}\right\}, \tag{48}$$

which, except for the slight difference in definition of the $\mathcal{M}$, has the same general form as Eq. (39). In particular, the two equations predict that orientation for large values of j can only be obtained by simultaneous excitation of states with different helicities ($\mathcal{M}_{\Omega_i}$ and $\mathcal{M}_{\Omega_i \pm 1}$).

V. APPLICATION TO ICN

Recently orientation of the rotational angular momentum of a molecular photofragment has been observed for the first time.[11] The system was ICN excited in its first absorption continuum by 249 nm circularly polarized light. The ICN A continuum has been studied by many different experimental techniques[22–44] and theoretical calculations.[45–69] Two product channels are open at the excitation wavelength of the experiments,

$$\text{ICN} + \hbar\omega \rightarrow \text{I}^*(^2P_{1/2}) + \text{CN}(^2\Sigma) \rightarrow \text{I}(^2P_{3/2}) + \text{CN}(^2\Sigma) \tag{49}$$

the energy difference being 7063 cm^{-1} (see Fig. 1). Actual-

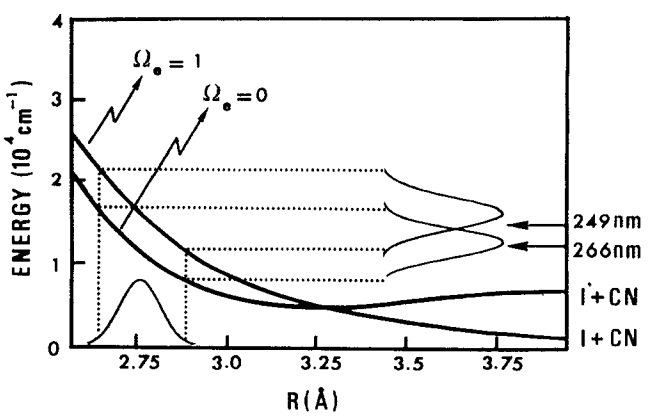

FIG. 1. Excited state potential energy curves for ICN in the collinear configuration for the two-state model. The curves are represented as a function of the distance R between the center of mass of CN and the iodine atom for a fixed CN distance of 1.17 Å. Also represented is the ground state wave function and the corresponding partial photodissociation cross sections for the two channels in the collinear configuration.

ly, since CN in the ground state has spin $\frac{1}{2}$ two electronic states corresponding to different total electronic angular momenta of the fragments, j are correlated to each one of the two limits. We have $\mathbf{j} = \mathbf{j}_I + \mathbf{s} + \mathbf{N}$, with $j_I = \frac{1}{2}$ for $I^*(^2P_{1/2})$, and $j_I = \frac{3}{2}$ for $I(^2P_{3/2})$, $s = \frac{1}{2}$ being the CN spin, and $\mathbf{N}$ the rotational angular momentum of the CN fragment. Since the CN fragments are predominantly found in medium to high $N \simeq 50$ rotational states,[39] it is possible to neglect j_I and s with respect to N in all the angular momentum coupling coefficients and simply identify $j \equiv N$. Except for the very low N values the orientation will not be affected by this approximation. The ϕ fragment wave functions defined in Eq. (9) can then be written as

$$\phi_{j\Omega}(\{\mathbf{r}_{bf}\};R) = Y_{j(\Omega-\Omega_e)}(\theta,\phi)|\Omega_e\rangle, \tag{50}$$

where θ and ϕ are the polar angles of the CN internuclear axis r in the molecule-fixed frame, and $|\Omega_e\rangle$ is the electronic fragment wave function with Ω_e being the projection of the total electronic angular momentum on the body-fixed $\mathbf{R}$ axis. In addition, since experimentally very little vibrational excitation is observed,[32] we have frozen the CN internuclear distance at its equilibrium distance. It should be noted however, that there are very interesting dynamical effects associated to the vibrational excitation of CN,[29,32,39] which could be studied if potential energy surfaces including the CN vibrational dependence were available.

What we need now is to define the excited potential energy surfaces. Recently,[13] *ab initio* calculations for the ICN ground and excited electronic states in the region of the A continuum have been performed. According to these calculations, two electronic excited states are involved in the photofragmentation of ICN when excited in this energy region. The two states ($^3\Pi_{0^+}$ and $^1\Pi_1$) are bent and correlate (diabatically) to $I^*(^2P_{1/2})$ and $I(^2P_{3/2})$ fragments, respectively, with CN being in its ground electronic state (see Fig. 1). Thus, according to the notation of Eq. (50), the $^3\Pi_0^+$ and the $^1\Pi_1$ diabatic states correspond to $\Omega_e = 0$ and $\Omega_e = 1$ quantum numbers, respectively.

Using a two dimensional spline interpolation of the *ab initio* points calculated by Yabushita and Morokuma[13] we have constructed two diabatic potential energy surfaces. Contour plots of these two surfaces are presented in Fig. 2. Following Yabushita and Morokuma,[13] a linear model at the crossing has been used to calculate the coupling between the two surfaces. We have defined

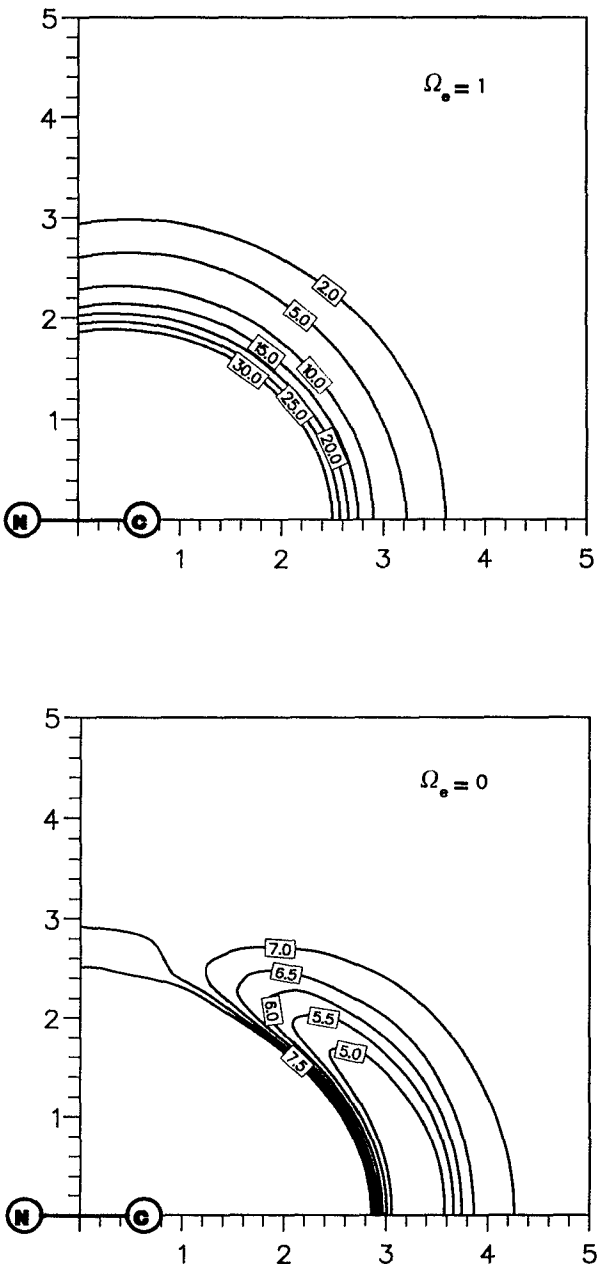

FIG. 2. Contour plots for the $\Omega_e = 0$ and $\Omega_e = 1$ potential energy surfaces for the two-state model. Energies are in 10^4 cm^{-1} and distances in Å.

$$V_{01}(R_{IC},\delta) = \begin{cases} V_0(R^*_{IC},\delta) - V_1(R^*_{IC},\delta) & |R_{IC} - R^*_{IC}| < 1.\ \text{a.u.} \\ [V_0(R^*_{IC},\delta) - V_1(R^*_{IC},\delta)]\, e^{-(|R_{IC}-R^*_{IC}|-1.)} & |R_{IC} - R^*_{IC}| \geqslant 1.\ \text{a.u.} \end{cases}, \tag{51}$$

with R_{IC} denoting the C–I distance ($R^*_{IC} = 2.7$ Å, being the crossing point) and δ the bending angle. R_{IC} and δ are related to the Jacobi coordinates R and θ used in our calculations, by simple trigonometry.[53,54] A contour plot of the potential coupling is presented in Fig. 3. We shall refer to these potential energies and couplings as the two-state model.

Since for ICN the initial rotational state of the molecule is not supposed to play a significant role in the dissociation dynamics,[54] we have performed quantum calculations for the transition from the $J_i = 0$ level in the ground state to the $J = 1$ manifold in the excited states. We can therefore use the final expressions presented in Sec. III. The calculations have

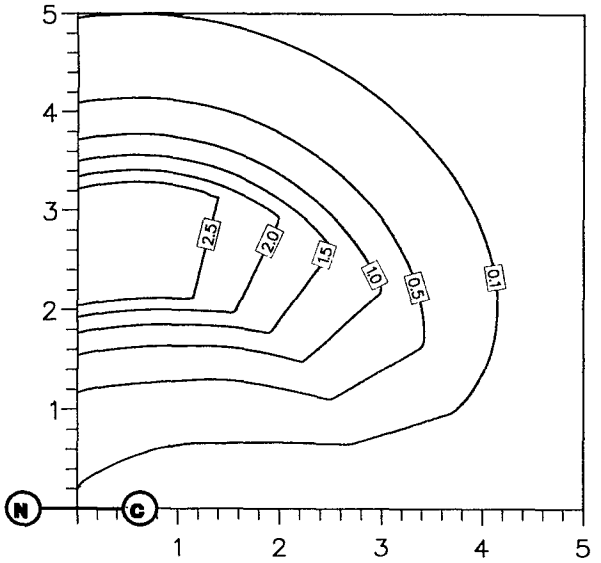

FIG. 3. Contour plot of the coupling potential between the $\Omega_e = 0$ and $\Omega_e = 1$ states for the two-state model. Energies are in 10^4 cm^{-1} and distances in Å.

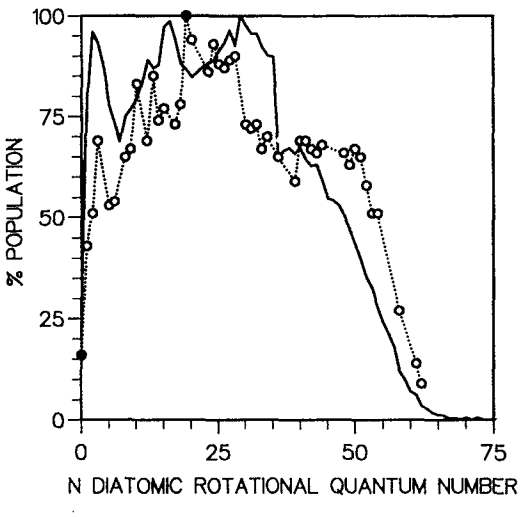

FIG. 4. The CN final state rotational distribution following photodissociation of ICN at 249 nm. The solid line represents the theoretical results obtained with the two-state model. The points are the experimental relative populations measured by O'Halloran *et al.* (Ref. 39).

been carried out as following. The initial ground state wave function (assuming $\Omega_e = 0$) has been computed using the formalism of Freed and co-workers.[52,53] The matrix elements defined in Eq. (35) have been obtained by solving the coupled equations (22) for the final dissociative wave functions, and evaluating the integral over R in the Franck–Condon approximation. We have neglected the Coriolis couplings between the $\Omega = 0$ and $\Omega = 1$ states induced by the $\mathbf{l}^2$ term in Eqs. (22). The number of coupled equations to be solved simultaneously is reduced by half when using this approximation. A preliminary test calculation has shown that the error introduced is of the order of 0.1% at the energy we are interested in ($\lambda = 249$ nm corresponds to 14 400 cm^{-1} excess energy with respect to the lower product channel). Two independent calculations are then performed, one for $\Omega = 0$ and another for $\Omega = 1$. Each one implies the resolution of about 170 coupled equations. The integration was performed from 2.5 to 10 Å in a grid of 1500 points. It should be noted that in the framework of the Coriolis decoupling approximation, the sum over Ω' in Eq. (35) reduce to only one term with $\Omega' = \Omega$. Since, in addition, $\Omega_i = 0$, we have $\Omega'_e = \Omega$ and this implies that the $\Omega = 0$ calculation corresponds to the dissociation dynamics associated to the parallel optical transition ($\Omega_e = 0$) while the $\Omega = 1$ calculation deals with the perpendicular transition $\Omega_e = 1$ only. This does not necessarily imply that the final Ω_e is unique for each one of these calculations. Since there are electronic transitions between the two surfaces, an initial parallel transition may produce both $\Omega_e = 0$ as well as $\Omega_e = 1$ channels (i.e., both I* and I atomic fragments).

Since the actual values of the electronic transition dipole moments $\mathscr{D}_0$ and $\mathscr{D}_1$ are not known we have determined *their* ratio by fitting the experimental iodine atoms electronic branching ratio $\mathrm{I}^*/(\mathrm{I} + \mathrm{I}^*) = 0.43$.[38,44] We have found good agreement between theory and experiment with $|\mathscr{D}_0/\mathscr{D}_1|^2 = 2$. In Fig. 4 we present the calculated and observed[39] final rotational state distribution of the CN fragments for excitation at 249 nm. Rather good agreement is obtained. The mechanism for the production of this rotational distribution proposed by Yabushita and Morokuma[13] is borne out by our calculations. Since the $\Omega_e = 0$ state has the most favorable Franck–Condon factors and it correlates to $\mathrm{I}^*(^2P_{1/2})$ in the collinear configuration, the CN fragments with low rotational excitation (i.e., those which dissociate collinearly) are associated with $\mathrm{I}^*(^2P_{1/2})$. On the other hand, those produced with intermediate and high N values are the result of transitions from one surface to the other in the bent configuration.

We turn now to the determination of the orientation of the CN rotational angular momentum. Experimentally the orientation has been measured for all CN fragments irrespective of the atomic iodine state.[11] In order to compare with experiments we then need to average our calculated individual orientations over the I* and I branching ratios. The results are presented in Fig. 5 together with the experimental points.[11] We note that although the overall behavior of the orientation as a function of N is qualitatively reproduced by the calculations, quantitatively the agreement is not very good, in particular for large N. The reason for this discrepancy could be due to the inaccuracy of the extrapolated potential energy surfaces at angles far from the collinear configuration. Highly rotationally excited fragments, for instance, are likely to explore the potential energy surfaces at large bending angles, where there are no *ab initio* points available. Also, the angular dependence of the coupling between the two dissociative electronic surfaces is very important in determining the orientation. It is clear that the model coupling we have used is not accurate enough and more *ab initio* points are needed to improve the two-state model.

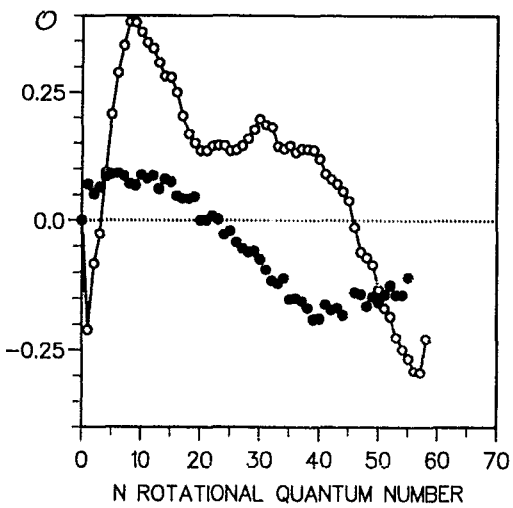

FIG. 5. The degree of orientation of the rotational angular momentum N of the CN fragments vs N. The theoretical results (solid line) correspond to the two-state model calculations. The experimental points (in black) are those of Hasselbrink *et al.* (Ref. 11).

We have also studied a three-state model which has been proposed recently by Black, Waldeck, and Zare.[44] The three surfaces are labeled with the quantum numbers $\Omega_e = 0$, 1, and 2. The $\Omega_e = 0$ surface is optically connected from the ground state and correlates to $I^*(^2P_{1/2})$ fragments. It is coupled to the optically inactive $\Omega_e = 2$ surface which correlates to $I(^2P_{3/2})$ fragments. These surfaces have been considered before by Goldfield, Houston, and Ezra[61] who performed classical trajectory calculations to study the final state rotational distribution of the CN fragments. Black *et al.*[44] have found that in order to reconcile all the experimental observations at 249 nm, it was necessary to consider a third state with $\Omega_e = 1$ carrying oscillator strength from the ground state. This state will then be responsible for the perpendicular component observed in the angular distribution of the $I(^2P_{3/2})$ fragments at low N.[44] Therefore, it was assumed that this state is correlated to the $I(^2P_{3/2})$ channel and that it is uncoupled to the other two states. We have chosen functional forms for the potential energy surfaces and couplings very similar to those used by Goldfield *et al.*,[61] namely,

$$\begin{aligned}
\langle 0|H_{\rm el}|0\rangle &= A_{00}e^{-\alpha_{00}R} - C_6/R^6 + B_{00}\theta^4 e^{-\beta_{00}R} \\
&\quad + 7063\ \text{cm}^{-1}, \\
\langle 2|H_{\rm el}|2\rangle &= A_{22}e^{-\alpha_{22}R}e^{-\gamma_{22}\theta^2} + B_{22}\theta^2 e^{-\beta_{22}R}, \\
\langle 1|H_{\rm el}|1\rangle &= A_{11}e^{-\alpha_{11}R}e^{-\gamma_{11}\theta^2} + B_{11}e^{-\beta_{11}R}e^{-\gamma_{11}(\theta-\pi)^2}, \\
\langle 0|H_{\rm el}|2\rangle &= A_{02}e^{-\alpha_{02}R}\theta^2 e^{-\gamma_{02}(\theta-\pi/12)^2}, \\
\langle 0|H_{\rm el}|1\rangle &= \langle 1|H_{\rm el}|2\rangle = 0. \qquad (52)
\end{aligned}$$

All the parameters are listed in Table I. They have been adjusted such that the final rotational distribution of CN agrees with the experimental results (see Fig. 6). Using these potentials we have calculated the degree of orientation of the CN fragments as a function of N. The results are presented in Fig. 7 together with the experimental results. We note that the three states model also reproduce qualitatively the behavior of the orientation as a function of the rotational quantum number. It is therefore possible to build several different models which can equally well explain the production of highly oriented fragments for large N. On the other hand, we have found in our calculations that the actual value of the orientation is very sensitive to details of the potential energy surfaces and couplings and that two models which can both reproduce very well the rotational distribution can give very different degrees of orientation.

TABLE I. Parameters of the potentials for the three-state model.

	0-0	0-2	2-2	1-1
A (cm^{-1})	1.331 + 14	5. + 8	2. + 10	5. + 11
B (cm^{-1})	3.4 + 18	···	1.49 + 10	3.5 + 9
α (Å^{-1})	8.5	3.35	5.	6.05
β (Å^{-1})	12.32	···	5.1	4.5
γ	···	50.	10.	5.
C_6 ($\text{cm}^{-1}\,\text{Å}^6$)	1.92 + 6	···	···	···

VI. CONCLUSIONS

We have studied the degree of orientation of molecular photofragments produced in highly excited rotational states. We have shown that the degree of orientation can be unexpectedly large if two or more helicity continua correlating to the same final states of the fragments are excited simultaneously. The helicity is associated to the projection Ω of $\mathbf{j}$ onto the dissociation coordinate $\mathbf{R}$ joining the center of mass of the fragments. The simultaneous excitation of continua with different helicity can be achieved in many different ways. If only one excited electronic manifold is populated, then in the framework of the Franck–Condon approximation we require that the transition dipole moment should

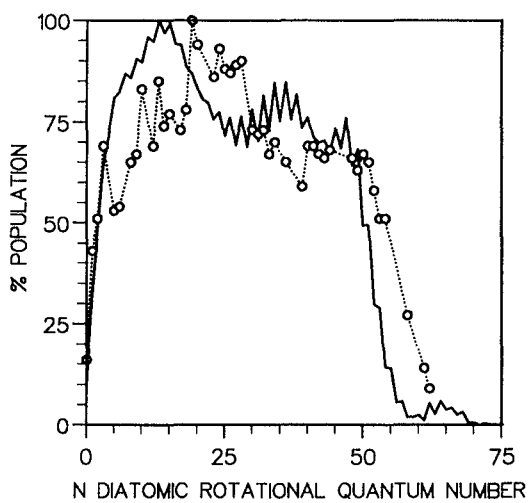

FIG. 6. Same as Fig. 4 for the three-state model.

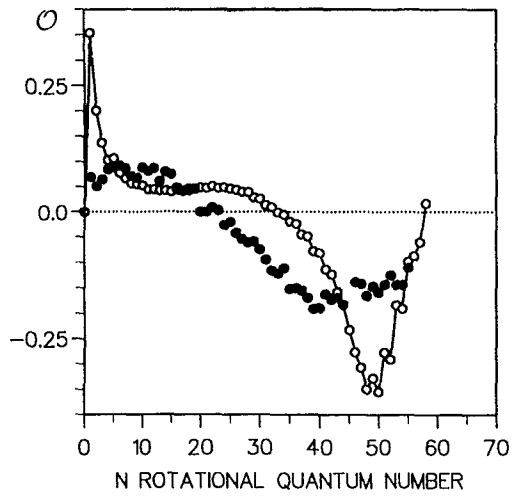

FIG. 7. Same as Fig. 5 for the three-state model.

have parallel and perpendicular components onto **R**. For nonlinear molecules this is likely to be the rule. For a bent triatomic molecule, for instance, the transition dipole moment should be in the plane of the molecule forming an angle different from 0 and $\pi/2$ with respect to **R**. A typical example is provided by NOCl which in the region 620–180 nm has transition dipole moments very nearly parallel to the NCl bond[70]

For linear molecules (such as ICN), it is clear that the transition dipole moment lies parallel or perpendicular to **R** in the collinear configuration. Hence, with only one surface orientation for large j can only be obtained through mixing with another surface of different symmetry. This mixing can only exist out of the collinear configuration and thus for linear molecules it is the contribution of the zero-point bending vibration of the ground state which is responsible for the orientation. This is the mechanism discussed by Vigué *et al.*[12]

Other possible mechanisms for linear triatomic molecules have been studied in this paper. If two excited electronic states with different symmetry (one parallel and the other one perpendicular) are optically connected to the ground state, simultaneous excitation of two helicity states can be obtained (provided the Franck–Condon factors are favorable). This is the situation encountered in the two-state model of ICN advanced by Morokuma and Nabushita.[13] Although the two states are correlated to different final states of the fragments (I + CN and I* + CN), transitions can occur in the crossing region when the molecule is bent. This ensures that the same final state of the fragments can be obtained with two different helicity states. The two-state model of Morokuma and Yabushita[13] and the mixing mechanism advanced by Vigué *et al.*,[12] are in fact intimately connected. If the crossing point between the two surfaces occurs near the Franck–Condon region, the adiabatic surfaces will then have the mixed transition dipole moment assumed by Vigué *et al.* This situation is likely to be found in many systems.

In the case of the three-state model proposed by Black *et al.*,[44] one of the final states (I + CN) can be produced by simultaneous excitation of the states with $\Omega_e = 0$ and $\Omega_e = 1$. Thus this channel shows orientation for large j while the other one corresponding to I* + CN has vanishingly small orientation for large j. By measuring selectively the degree of orientation in coincidence with the final state of the iodine atom it would be possible to discriminate between these two models. Another important conclusion of this work is that the degree of orientation is very sensitive to the details of the potential energy surfaces and couplings. In particular, we have found that the two models studied here reproduce very well the fragments' rotational distribution and yet give very different orientational values.

Finally, it should be noted that the mechanisms considered here for ICN can apply as well to other systems dissociating into two fragments. In particular, the ClCN and BrCN molecules for which there is now experimental and theoretical information available[71,72] should be amenable to very similar theoretical treatment. Another very interesting system in this context is OCS for which it has been demonstrated that parallel and perpendicular transitions are simultaneously present at a variety of excitation wavelengths.[73]

ACKNOWLEDGMENTS

We wish to thank Dr. Janet Waldeck and Professor R. N. Zare for very helpful discussions. The calculations presented here were carried out on the VP200 computer at CIRCE (Orsay).

APPENDIX: DERIVATION OF THE GENERAL EXPRESSIONS

We consider the general case where the two fragments A and B carry nonzero angular momenta j_A and j_B, respectively. The orientation and the alignment of fragment A will then be given by

$$\mathcal{O}^{(j_A)} \equiv \langle (j_A)_z / |\mathbf{j}_A| \rangle = \sum_{m_{j_A}} \frac{m_{j_A}}{\sqrt{j_A(j_A+1)}} \rho^{(j_A)}_{m_{j_A},m_{j_A}}, \tag{A1a}$$

$$\mathcal{A}^{(j_A)} \equiv \langle 3(j_A)_z^2 / |\mathbf{j}_A|^2 - 1 \rangle = \sum_{m_{j_A}} \left(\frac{3m_{j_A}^2}{j_A(j_A+1)} - 1 \right) \rho^{(j_A)}_{m_{j_A},m_{j_A}}, \tag{A1b}$$

where

$$\rho^{(j_A)}_{m_{j_A},m_{j_A}} = \sigma^{(j_A)}_{m_{j_A}} \Big/ \sum_{m_{j_A}} \sigma^{(j_A)}_{m_{j_A}} \tag{A2}$$

with

$$\sigma^{(j_A)}_{m_{j_A}} = \frac{4\pi^2\omega}{c} \sum_{j_B m_{j_B}} \sum_{\ell m_\ell} |\langle \Psi_{j_A m_{j_A} j_B m_{j_B} \ell m_\ell} | \mathbf{d}\cdot\hat{\mathbf{e}} | \Psi_i \rangle|^2. \tag{A3}$$

Now

$$\Psi_{j_A m_{j_A} j_B m_{j_B} \ell m_\ell} = \sum_{j m_j} (-)^{j_A - j_B + m_j} (2j+1)^{1/2} \times \begin{pmatrix} j_A & j_B & j \\ m_{j_A} & m_{j_B} & -m_j \end{pmatrix} \Psi_{j_A j_B j m_j \ell m_\ell}, \quad \text{(A4)}$$

where $\mathbf{j} = \mathbf{j}_A + \mathbf{j}_B$ is the total angular momentum of the fragments and $\Psi_{j_A j_B j m_j \ell m_\ell}$ is the wave function defined asymptotically as in Eq. (5). Introducing now the total angular momentum $\mathbf{J} = \mathbf{j} + \mathbf{l}$ and the body-fixed wave functions defined in Eqs. (8) and (9), we obtain

$$\sigma^{(j_A)}_{m_{j_A}} = \frac{4\pi^2\omega}{c} \sum_{j_B m_{j_B}} \sum_{j m_j} \sum_{j' m_{j'}} \sum_{\ell m_\ell} \sum_{\Omega J M} \sum_{\Omega' J' M'} (-)^{M + M' - \Omega - \Omega' + 2j_A - 2j_B + m_j + m_{j'}} \times (2\ell+1)(2J+1)^{1/2}(2J'+1)^{1/2}(2j+1)^{1/2}(2j'+1)^{1/2} \times \begin{pmatrix} j & \ell & J \\ \Omega & 0 & -\Omega \end{pmatrix} \begin{pmatrix} j & \ell & J \\ m_j & m_\ell & -M \end{pmatrix} \begin{pmatrix} j & \ell & J \\ \Omega & 0 & -\Omega \end{pmatrix} \begin{pmatrix} j' & \ell & J' \\ m_{j'} & m_\ell & -M' \end{pmatrix} \times \begin{pmatrix} j_A & j_B & j \\ m_{j_A} & m_{j_B} & -m_j \end{pmatrix} \begin{pmatrix} j_A & j_B & j' \\ m_{j_A} & m_{j_B} & -m_{j'} \end{pmatrix} \langle \Psi_i | \mathbf{d}\cdot\hat{\mathbf{e}} | \Psi_{j_A j_B j \Omega J M} \rangle^* \langle \Psi_i | \mathbf{d}\cdot\hat{\mathbf{e}} | \Psi_{j_A j_B j' \Omega' J' M'} \rangle. \quad \text{(A5)}$$

We now prove a useful relation between the Wigner coefficients. We start with [see Eq. (4.16) in Ref. 15]

$$\begin{pmatrix} j_1 & j_2 & j_3 \\ m_1 & m_2 & -m_3 \end{pmatrix} \begin{pmatrix} j_4 & j_5 & j_3 \\ m_4 & m_5 & m_3 \end{pmatrix} = \sum_{j_6} (2j_6+1)(-)^{j_1 + j_2 - j_3 + j_4 + j_5 j_6 - m_1 - m_4} \times \begin{Bmatrix} j_1 & j_2 & j_3 \\ j_4 & j_5 & j_6 \end{Bmatrix} \begin{pmatrix} j_5 & j_1 & j_6 \\ m_5 & m_1 & m_6 \end{pmatrix} \begin{pmatrix} j_2 & j_4 & j_6 \\ m_2 & m_4 & -m_6 \end{pmatrix}. \quad \text{(A6)}$$

From Eq. (6) we can write

$$\sum_{j_3} (2j_3+1) \begin{pmatrix} j_1 & j_2 & j_3 \\ M_1 & M_2 & -M_3 \end{pmatrix} \begin{pmatrix} j_4 & j_5 & j_3 \\ M_4 & M_5 & M_3 \end{pmatrix} \begin{pmatrix} j_1 & j_2 & j_3 \\ m_1 & m_2 & -m_3 \end{pmatrix} \begin{pmatrix} j_4 & j_5 & j_3 \\ m_4 & m_5 & m_3 \end{pmatrix} = \sum_{j_6} (2j_6+1)(-)^{j_1 + j_2 + j_4 + j_5 j_6 - m_1 - m_4} \begin{pmatrix} j_5 & j_1 & j_6 \\ m_5 & m_1 & m_6 \end{pmatrix} \begin{pmatrix} j_2 & j_4 & j_6 \\ m_2 & m_4 & -m_6 \end{pmatrix} \times \sum_{j_3} (2j_3+1)(-)^{-j_3} \begin{Bmatrix} j_1 & j_2 & j_3 \\ j_4 & j_5 & j_6 \end{Bmatrix} \begin{pmatrix} j_1 & j_2 & j_3 \\ M_1 & M_2 & -M_3 \end{pmatrix} \begin{pmatrix} j_4 & j_5 & j_3 \\ M_4 & M_5 & M_3 \end{pmatrix} \quad \text{(A7)}$$

and using again Eq. (A6) we obtain

$$\sum_{j_3} (2j_3+1) \begin{pmatrix} j_1 & j_2 & j_3 \\ m_1 & m_2 & -m_3 \end{pmatrix} \begin{pmatrix} j_1 & j_2 & j_3 \\ M_1 & M_2 & -M_3 \end{pmatrix} \begin{pmatrix} j_4 & j_5 & j_3 \\ m_4 & m_5 & m_3 \end{pmatrix} \begin{pmatrix} j_4 & j_5 & j_3 \\ M_4 & M_5 & M_3 \end{pmatrix} = \sum_{j_6} (2j_6+1)(-)^{2j_6 - m_1 - m_4 + M_1 + M_4} \begin{pmatrix} j_5 & j_1 & j_6 \\ m_5 & m_1 & m_6 \end{pmatrix} \begin{pmatrix} j_5 & j_1 & j_6 \\ M_5 & M_1 & -M_6 \end{pmatrix} \begin{pmatrix} j_2 & j_4 & j_6 \\ m_2 & m_4 & -m_6 \end{pmatrix} \begin{pmatrix} j_2 & j_4 & j_6 \\ M_2 & m_4 & M_6 \end{pmatrix}. \quad \text{(A8)}$$

Using now Eq. (A8) into Eq. (A5), we can write

$$\sigma^{(j_A)}_{m_{j_A}} = \frac{4\pi^2\omega}{c} \sum_{j_B m_{j_B}} \sum_{j m_j} \sum_{j' m_{j'}} (-)^{2j_A - 2j_B + m_j + m_{j'}} (2j+1)^{1/2}(2j'+1)^{1/2} \times \begin{pmatrix} j_A & j_B & j \\ m_{j_A} & m_{j_B} & -m_j \end{pmatrix} \begin{pmatrix} j_A & j_B & j' \\ m_{j_A} & m_{j_B} & -m_{j'} \end{pmatrix} \sum_K (2K+1)(-)^{2K - m_{j'}} \begin{pmatrix} j & j' & K \\ -m_j & m_{j'} & (m_j - m_{j'}) \end{pmatrix} \times \sum_{\Omega J M} \sum_{\Omega' J' M'} (-)^{M' - 2\Omega - 2\Omega'} (2J+1)^{1/2}(2J'+1)^{1/2} \begin{pmatrix} J & J' & K \\ -\Omega & \Omega' & (\Omega - \Omega') \end{pmatrix} \begin{pmatrix} J' & J & K \\ -M' & M & (M - M') \end{pmatrix} \times \begin{pmatrix} j' & j & K \\ -\Omega' & \Omega & (\Omega' - \Omega) \end{pmatrix} \langle \Psi_i | \mathbf{d}\cdot\hat{\mathbf{e}} | \Psi_{j_A j_B j \Omega J M} \rangle^* \langle \Psi_i | \mathbf{d}\cdot\hat{\mathbf{e}} | \Psi_{j_A j_B j' \Omega' J' M'} \rangle \quad \text{(A9)}$$

and using [see Eq. (4.15) in Ref. 15]

$$\sum_{m_2 m_3 m_4} (-)^{j_1 + j_2 - j_3 + j_4 + j_5 j_6 - m_1 - m_4} \begin{pmatrix} j_1 & j_2 & j_3 \\ m_1 & m_2 & -m_3 \end{pmatrix} \begin{pmatrix} j_4 & j_5 & j_3 \\ m_4 & m_5 & m_3 \end{pmatrix} \begin{pmatrix} j_2 & j_4 & j_6 \\ m_2 & m_4 & -m_6 \end{pmatrix} = \begin{Bmatrix} j_1 & j_2 & j_3 \\ j_4 & j_5 & j_6 \end{Bmatrix} \begin{pmatrix} j_5 & j_1 & j_6 \\ m_5 & m_1 & m_6 \end{pmatrix}, \quad \text{(A10)}$$

we obtain

$$\sigma_{m_{j_A}}^{(j_A)} = \frac{4\pi^2\omega}{c} \sum_K (-)^{j_A - m_{j_A}} \frac{(2K+1)}{\sqrt{2j_A+1}} \begin{pmatrix} j_A & j_A & K \\ m_{j_A} & -m_{j_A} & 0 \end{pmatrix} T_K^{(j_A)}, \tag{A11}$$

with

$$T_K^{(j_A)} = \sum_{j_B j j'} \sum_{\Omega J} \sum_{\Omega' J'} \sum_M (-)^{-j_A - j_B + M} (2j_A+1)^{1/2} \begin{Bmatrix} j_A & j_A & K \\ j & j' & j_B \end{Bmatrix} (2j+1)^{1/2} (2j'+1)^{1/2} \begin{pmatrix} j' & j & K \\ -\Omega' & \Omega & (\Omega'-\Omega) \end{pmatrix}$$

$$\times (2J+1)^{1/2} (2J'+1)^{1/2} \begin{pmatrix} J & J' & K \\ -\Omega & \Omega' & (\Omega-\Omega') \end{pmatrix} \begin{pmatrix} J' & J & K \\ -M & M & 0 \end{pmatrix} \langle \Psi_i | \mathbf{d}\cdot\hat{\mathbf{e}} | \Psi_{j_A j_B j \Omega J M} \rangle^* \langle \Psi_i | \mathbf{d}\cdot\hat{\mathbf{e}} | \Psi_{j_A j_B j \Omega' J' M'} \rangle, \tag{A12}$$

which for $j_B = 0$ reduce to Eqs. (14) and (15).

Introducing now into Eq. (A12) the matrix elements defined in Eq. (25), averaging over M_i since we assume the molecule is initially randomly oriented, and using Eq. (A10), we finally get

$$T_K^{(j_A)} = -F_K(\hat{\mathbf{e}}) \sum_{j_B j j'} \sum_{\Omega J} \sum_{\Omega' J'} (-)^{-j_A - j_B - J_i - K} (2j_A+1)^{1/2} \begin{Bmatrix} j_A & j_A & K \\ j & j' & j_B \end{Bmatrix}$$

$$\times (2j+1)^{1/2} (2j'+1)^{1/2} \begin{pmatrix} j' & j & K \\ -\Omega' & \Omega & (\Omega'-\Omega) \end{pmatrix} (2J+1)^{1/2} (2J'+1)^{1/2} \begin{pmatrix} J & J' & K \\ \Omega & -\Omega' & (\Omega'-\Omega) \end{pmatrix}$$

$$\times \begin{Bmatrix} 1 & 1 & K \\ J & J' & j_i \end{Bmatrix} \langle J_i \| \mathbf{d} \| j_A j_B j \Omega J \rangle^* \langle J_i \| \mathbf{d} \| j_A j_B j \Omega' J' \rangle, \tag{A13}$$

which reduces to Eq. (29) when $j_B = 0$.

In the axial recoil limit, we can replace the reduced matrix elements $\langle J_i \| \mathbf{d} \| j_A j_B j \Omega J \rangle$ by Eq. (44) in which case, using Eq. (A6) together with the normalization of the Wigner coefficients, Eq. (A13) can be recast in the form

$$T_K^{(j_A)} = -F_K(\hat{\mathbf{e}}) \sum_{j_B j j'} \sum_{\Omega\Omega'} \sum_{\Omega_i} (-)^{-j_A - j_B + \Omega + \Omega' - \Omega_i - K} (2j_A+1)^{1/2} \begin{Bmatrix} j_A & j_A & K \\ j & j' & j_B \end{Bmatrix}$$

$$\times (2j+1)^{1/2} (2j'+1)^{1/2} \begin{pmatrix} j' & j & K \\ -\Omega & \Omega' & (\Omega-\Omega') \end{pmatrix}$$

$$\times \begin{pmatrix} 1 & 1 & K \\ -(\Omega_i - \Omega') & (\Omega - \Omega_i) & (\Omega' - \Omega) \end{pmatrix} \mathscr{M}_{\Omega}^{(j_A j_B j)^*}(\Omega_i, J_i) \mathscr{M}_{\Omega'}^{(j_A j_B j)}(\Omega_i, J_i), \tag{A14}$$

which reduces to Eq. (46) when $j_B = 0$ or when j_B is much smaller than j_A.

[1] See, for instance, the contributions on photodissociation, in Proceedings of Faraday Symposium 24, J. Chem. Soc. Faraday Trans. II Mol. Chem. Phys. **85** (1989).
[2] O. S. Vasyutinskii, Sov. Phys. JETP Lett. **31**, 428 (1980); Opt. Spectrosc. (U.S.S.R) **51**, 124 (1980).
[3] O. S. Vasyutinskii, Z. Phys D **15**, 105 (1990).
[4] J. Vigué, P. Grangier, G. Roger, and A. Aspect, J. Phys. Lett. **42**, L531 (1981).
[5] J. Vigué, J. A. Beswick, and M. Broyer, J. Phys. (Paris) **44**, 1225 (1983).
[6] S. J. Singer, K. F. Freed, and Y. B. Band, J. Chem. Phys. **79**, 6060 (1983).
[7] Y. B. Band, K. F. Freed, and S. J. Singer, J. Chem. Phys. **84**, 3762 (1986).
[8] M. Glass-Maujean and J. A. Beswick, Phys. Rev. A **36**, 1160 (1987).
[9] M. Glass-Maujean and J. A. Beswick, Phys. Rev. A **38**, 5660 (1988).
[10] M. Glass-Maujean and J. A. Beswick, in Ref. 1, p. 983.
[11] E. Hasselbrink, J. R. Waldeck, and R. N. Zare, Chem. Phys. **126**, 191 (1988).
[12] J. Vigué, B. Girard, G. Gouédard, and N. Billy, Phys. Rev. Lett. **62**, 1358 (1989).
[13] S. Yabushita and K. Morokuma, Chem. Phys. Lett. **175**, 518 (1990).
[14] C. H. Greene and R. N. Zare, Annu. Rev. Phys. Chem. **33**, 119 (1982).
[15] R. N. Zare, *Angular Momentum: Understanding Spatial Aspects in Chemistry and Physics* (Addison Wesley, New York, 1988).
[16] M. Shapiro and G. G. Balint-Kurti, Chem. Phys. **61**, 137 (1981).
[17] M. Shapiro and G. G. Balint-Kurti, in *Photodissociation and Photoionization*, edited by K. P. Lawley (Wiley, New York, 1985).
[18] S. J. Singer, K. F. Freed, and Y. B. Band, Adv. Chem. Phys. **61**, 1 (1985).
[19] K. Blum, *Density Matrix Theory and Applications* (Plenum, New York, 1981).
[20] N. A. Cherepkov, Adv. At. Mol. Phys. **19**, 395 (1983).
[21] U. Heinzmann, in *Applications of Circularly Polarized Radiation Using Synchrotron Radiation and Ordinary Sources*, edited by F. Allen and C. Bustamante (Plenum, New York, 1985).
[22] G. W. King and A. W. Richardson, J. Mol. Spectrosc. **21**, 339 (1966).
[23] J. H. Ling and K. R. Wilson, J. Chem. Phys. **63**, 101 (1975).
[24] A. P. Baronavski and J. R. McDonald, Chem. Phys. Lett. **45**, 172 (1977).
[25] M. J. Sabety-Dzvonik and R. J. Cody, J. Chem. Phys. **66**, 125 (1977).
[26] W. M. Pitts and A. P. Baronavski, Chem. Phys. Lett. **71**, 395 (1980).
[27] W. Krieger, J. Häger, and J. Pfab, Chem. Phys. Lett. **85**, 69 (1982).
[28] A. P. Baronavski, Chem. Phys. **66**, 217 (1982).
[29] W. H. Fisher, T. Carrington, S. V. Filseth, C. M. Sadowski, and C. H.

Dugan, Chem. Phys. **82**, 443 (1983).
[30] I. Nadler, H. Reisler, and C. Wittig, Chem. Phys. Lett. **103**, 451 (1984).
[31] W. H. Fisher, R. Eng, T. Carrington, C. H. Dugan, S. V. Filseth, and C. M. Sadowski, Chem. Phys. **89**, 457 (1984).
[32] W. J. Marinelli, N. Sivakumar, and P. L. Houston, J. Phys. Chem. **88**, 6685 (1984).
[33] F. Shokoohi, S. Hay, and C. Wittig, Chem. Phys. Lett. **110**, 1 (1984).
[34] I. Nadler, D. Mahgerefteh, H. Reisler, and C. Witting, J. Chem. Phys. **82**, 3885 (1985).
[35] J. L. Knee, L. R. Khundar, and A. H. Zewail, J. Phys. Chem. **89**, 4659 (1985).
[36] N. F. Scherer, J. L. Knee, D. D. Smith, and A. H. Zewail, J. Phys. Chem. **89**, 5141 (1985).
[37] G. E. Hall, N. Sivakumar, and P. L. Houston, J. Chem. Phys. **84**, 2120 (1986).
[38] W. P. Hess and S. R. Leone, J. Chem. Phys. **86**, 3773 (1987).
[39] M. A. O'Halloran, H. Joswig, and R. N. Zare, J. Chem. Phys. **87**, 303 (1987).
[40] (a) M. Dantus, M. J. Rosker, and A. H. Zewail, J. Chem. Phys. **87**, 2395 (1987); (b) **89**, 6128 (1988); (c) A. H. Zewail, in Ref. 1, p. 1221.
[41] J. F. Black, J. R. Waldeck, E. Hasselbrink, and R. N. Zare, in Ref. 1, p. 1044 and 1312.
[42] A. Paul, W. H. Fink, and W. M. Jackson, Chem. Phys. Lett. **153**, 121 (1988).
[43] J. F. Black, E. Hasselbrink, J. R. Waldeck, and R. N. Zare, Mol. Phys. **71**, 1143 (1990).
[44] J. F. Black, J. R. Waldeck, and R. N. Zare, J. Chem. Phys. **92**, 3519 (1990).
[45] K. E. Holdy, L. C. Klotz, and K. R. Wilson, J. Chem. Phys. **52**, 4588 (1970).
[46] M. Shapiro and R. D. Levine, Chem. Phys. Lett. **5**, 499 (1970).
[47] A. D. Wilson and R. D. Levine, Mol. Phys. **27**, 1197 (1974).
[48] M. D. Morse, K. F. Freed, and Y. B. Band, Chem. Phys. Lett. **44**, 125 (1976).
[49] U. Halavee and M. Shapiro, Chem. Phys. **21**, 105 (1977).
[50] J. A. Beswick and J. Jortner, Chem. Phys. **24**, 1 (1977).
[51] M. N. R. Ashfold and J. P. Simons, J. Chem. Soc. Faraday Trans. 2 **74**, 280 (1978).
[52] Y. B. Band and K. F. Freed, J. Chem. Phys. **70**, 3620 (1979).
[53] (a) M. D. Morse, K. F. Freed, and Y. B. Band, J. Chem. Phys. **70**, 3604 (1979); (b) **70**, 3620 (1979).
[54] J. A. Beswick and W. M. Gelbart, J. Phys. Chem. **84**, 3148 (1980).
[55] M. D. Morse and K. F. Freed, J. Chem. Phys. **74**, 4395 (1981).
[56] R. W. Heather and J. C. Light, J. Chem. Phys. **78**, 5513 (1983).
[57] (a) M. D. Pattengill, Chem. Phys. **78**, 229 (1983); (b) **87**, 419 (1984).
[58] B. A. Waite, H. Helvajian, B. I. Dunlap, and I. Baronavski, Chem. Phys. Lett. **111**, 544 (1984).
[59] R. Schinke and V. Engel, J. Chem. Phys. **83**, 5068 (1985).
[60] W. Boyd, A. Waite, and B. I. Dunlap, J. Chem. Phys. **84**, 1391 (1986).
[61] E. M. Goldfield, P. L. Houston, and G. S. Ezra, J. Chem. Phys. **84**, 3120 (1986).
[62] H. Joswig, M. A. O'Halloran, R. N. Zare, and M. S. Child, Faraday Discuss. Chem. Soc. **82**, 79 (1986).
[63] (a) C. H. Dugan and D. Anthony, J. Phys. Chem. **91**, 3929 (1987); (b) C. H. Dugan, *ibid.* **92**, 720 (1988).
[64] S. O. Williams and D. G. Imre, J. Phys. Chem. **92**, 6648 (1988).
[65] I. Benjamin and K. R. Wilson, J. Chem. Phys. **90**, 4176 (1989).
[66] R. Heather and H. Metiu, Chem. Phys. Lett. **157**, 505 (1989).
[67] M. Jacon, O. Atabek, and C. Leforestier, J. Chem. Phys. **91**, 1585 (1989).
[68] N. E. Henriksen and E. J. Heller, J. Chem. Phys. **91**, 4700 (1989).
[69] H. Guo and G. C. Schatz, J. Chem. Phys. **92**, 1634 (1990).
[70] Y. Y. Bai, A. Ogai, C. X. W. Qian, L. Iwata, G. A. Segal, and H. Reisler, J. Chem. Phys. **90**, 3903 (1989).
[71] Y. Y. Bai, G. A. Segal, and H. Reisler, J. Chem. Phys. **94**, 331 (1991).
[72] E. A. J. Wannenmacher, H. Lin, W. H. Fink, A. J. Paul, and W. M. Jackson, J. Chem. Phys. **95**, 3431 (1991).
[73] G. E. Hall, N. Sivakumar, P. L. Houston, and I. Burak, Phys. Rev. Lett. **56**, 1671 (1986).